On numerical quadrature for C^1 quadratic Powell-Sabin 6-split macro-triangles

Michael Bartoň[a], Jiří Kosinka[b,*]

[a] *BCAM – Basque Center for Applied Mathematics, Alameda de Mazarredo 14, 48009 Bilbao, Basque Country, Spain*
[b] *Johann Bernoulli Institute, University of Groningen, Nijenborgh 9, 9747 AG, Groningen, the Netherlands*

Abstract

The quadrature rule of Hammer and Stroud [16] for cubic polynomials has been shown to be exact for a larger space of functions, namely the C^1 cubic Clough-Tocher spline space over a macro-triangle if and only if the split-point is the barycentre of the macro-triangle [21]. We continue the study of quadrature rules for spline spaces over macro-triangles, now focusing on the case of C^1 quadratic Powell-Sabin 6-split macro-triangles. We show that the 3-node Gaussian quadrature(s) for quadratics can be generalised to the C^1 quadratic Powell-Sabin 6-split spline space over a macro-triangle for a two-parameter family of inner split-points, not just the barycentre as in [21]. The choice of the inner split-point uniquely determines the positions of the edge split-points such that the whole spline space is integrated exactly by a corresponding polynomial quadrature. Consequently, the number of quadrature points needed to exactly integrate this special spline space reduces from twelve to three.

For the inner split-point at the barycentre, we prove that the two 3-node quadratic polynomial quadratures of Hammer and Stroud exactly integrate also the C^1 quadratic Powell-Sabin spline space if and only if the edge split-points are at their respective edge midpoints. For other positions of the inner and edge split-points we provide numerical examples showing that three nodes suffice to integrate the space exactly, but a full classification and a closed-form solution in the generic case remain elusive.

Keywords: Numerical integration, Powell-Sabin spline space, Gaussian quadrature rules

1. Introduction

Quadrature rules offer an elegant and efficient way to numerically evaluate integrals of functions from a linear space under consideration [18]. These rules typically require function evaluation at specific points, called *nodes*, and these values are multiplied by constants, called *weights*, to give the final value of the integral as a weighted sum. That is, one wishes to satisfy

$$\int_\Omega f(\mathbf{x})\,\mathrm{d}\mathbf{x} = \sum_{i=1}^{m} \omega_i f(\mathbf{t}_i) + R_m(f), \tag{1}$$

where $\Omega \subset \mathbb{R}^n$ is the domain of interest, m is the number of nodes (quadrature points), f is a function of n variables, i.e., $f : \mathbb{R}^n \to \mathbb{R}$, and $R_m(f)$ is the error term of the rule. Typically, the rule is required to be *exact*, that is, $R_m(f) \equiv 0$ for each element of a predefined linear function space $\mathcal{L}$. Moreover, the rule is said to be *Gaussian* if m is the *minimal* number of nodes $\mathbf{t}_i \in \mathbb{R}^n$ at which f has to be evaluated.

There is an extensive number of various quadrature rules depending on n (f is univariate [15], bivariate [28, 39], multivariate [16]), domain shape (disc, hypercube, simplex) [37], and the type of the linear

*Corresponding author
Email addresses: mbarton@bcamath.org (Michael Bartoň), j.kosinka@rug.nl (Jiří Kosinka)

space (polynomials [15], splines [4, 6, 29, 33], rational functions [38], smooth non-polynomial [7, 27]). For polynomial multivariate integration, the field is well studied and the reader is referred to [37].

In the univariate case, a lot of research has been devoted to piecewise polynomials to address integration for spline spaces arising in isogeometric analysis [10]. Hughes et al. [19] introduced so called half-point rule for splines that needs the minimum number of quadrature points. However, this rule is in general exact only over the whole real line (infinite domain). For finite domains, one may introduce additional quadrature points [2] which make the rule non-Gaussian (slightly sub-optimal in terms of the number of quadrature points), but more importantly, it yields quadrature weights that can be negative, unlike in Gaussian quadratures. When computing Galerkin approximations, assembling mass and stiffness matrices is the bottleneck of the whole computation and efficient quadrature rules for specific spline spaces are needed to efficiently evaluate the matrix entries [5, 6, 8, 17, 20].

In the multivariate case where spline spaces possess a tensor-product structure, univariate quadrature rules are typically used in each direction, resulting in tensor-product rules [17]. Recently, Calabrò et al. [8] have changed the paradigm of the mass and stiffness matrix computation from the traditional element-wise assembly to a row-wise concept. When building the mass matrix, one B-spline basis function of the scalar product involved is considered as a positive measure (i.e., a weight function), and a weighted quadrature with respect to that weight is computed for each matrix row. Such an approach brings significant computational savings because the number of quadrature points in each parameter dimension is independent on the polynomial degree and requires asymptotically (for a large number of elements) only two points per element. For the multivariate case that is unstructured such as triangular meshes in 2D, however, constructing efficient quadrature rules from tensor product counterparts is unnatural, resulting in rules that are often not symmetric even though they act on a symmetric domain [28].

Our research focuses on bivariate functions over triangular domains where the spline space is piecewise polynomial. Little attention has been given to this topic so far. The current state of the art of integration for spline spaces of this type, such as C^1 cubic Clough-Tocher macro-triangles [9] and various box-spline constructions [13], is to apply simplex quadrature [36] over each (micro-)simplex separately. Such integration is inefficient as it ignores the continuity of the spline functions across macro- and micro-elements. In a related line of research, work has been done on integration schemes based on quasi-interpolants over (refined) triangulations [12, 25, 31]; see also the survey [26]. Recently, we have shown that the quadrature rule of Hammer and Stroud [16] for cubic polynomials is exact for a larger space of functions, namely the C^1 cubic Clough-Tocher spline space over a macro-triangle, if and only if the split-point is the barycentre of the macro-triangle [21].

In the present paper, we continue the study of Gaussian quadrature rules for polynomial spline spaces over triangulations. We study the case of C^1 quadratic Powell-Sabin 6-split macro-triangles and show that the choice of generalisation of a polynomial rule that is exact for quadratic polynomials is a lot broader than its cubic counterpart studied in [21]. It is known that total-degree quadratic polynomials over triangles can be integrated using three quadrature points [37] and this number of points is optimal. However, the nine degrees of freedom (three nodes in 2D and three weights) admit a larger space for exact integration than the six-dimensional space of quadratics. We formulate algebraic conditions for the inner and edge split-points such that the underlying Powell-Sabin 6-split spline space is integrated exactly by the quadratic polynomial quadrature. This result allows us to efficiently integrate quadratic C^1 Powell-Sabin 6-split splines using only three nodes per macro-triangle, in contrast to traditional schemes using twelve nodes. Further, we provide numerical examples demonstrating that the generic case with arbitrary split-points is also covered by three nodes. However, a close-form solution remains a topic for future research.

The rest of the paper is organised as follows. We start by recalling some basic concepts such as Bézier triangles, the Powell-Sabin macro-triangle, and simplectic quadrature for quadratic polynomials in Section 2. This is followed by Section 3, where we state and prove our main result regarding Gaussian quadrature for C^1 quadratic Powell-Sabin macro-triangles, and demonstrate it on numerical examples. Finally, we conclude the paper in Section 4.

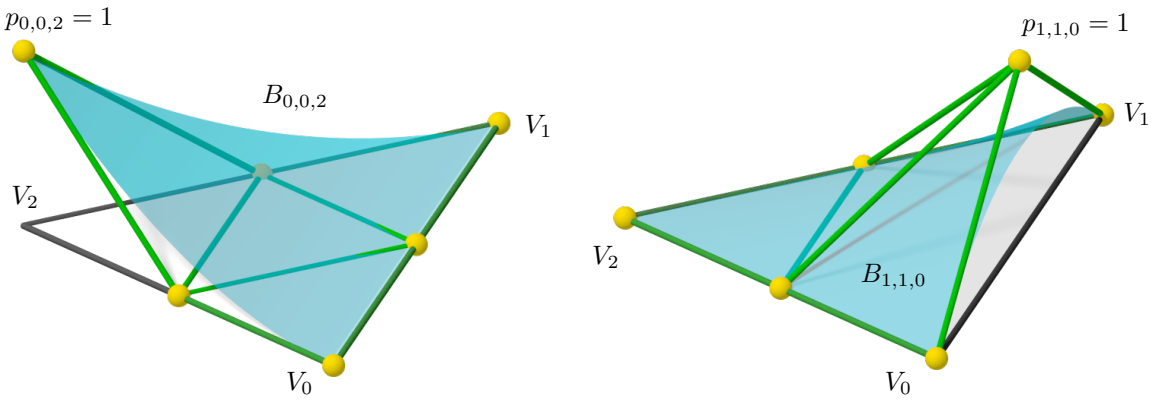

Figure 1: Two quadratic Bernstein basis functions (transparent blue) over $\mathcal{T} = (V_0V_1V_2)$ and their control nets (green) are shown.

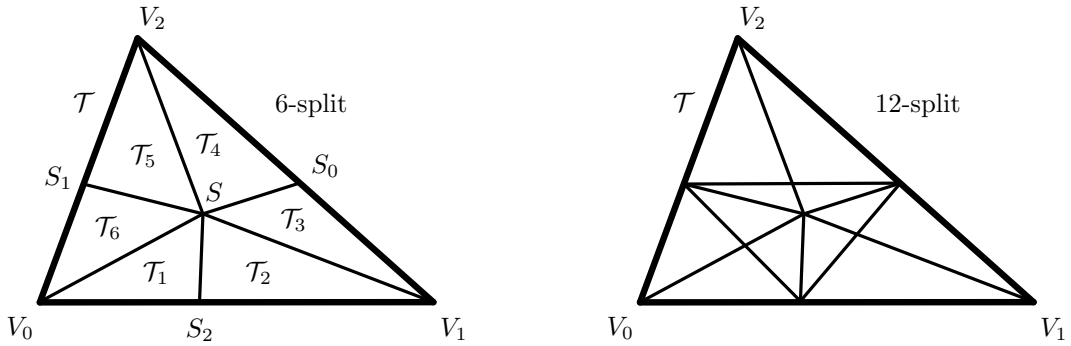

Figure 2: The Powell-Sabin 6-split (left) and 12-split (right).

2. Preliminaries

We first introduce some basic concepts of Bézier triangles and the C^1 quadratic Powell-Sabin 6-split, and then recall Hammer-Stroud quadratures for quadratic triangular polynomials.

2.1. Bézier triangles

Consider a non-degenerate triangle $\mathcal{T}$ given by three vertices V_0, V_1, and V_2 in $\mathbb{R}^2$. We assume that the area of $\mathcal{T}$ is equal to one, otherwise one can scale it accordingly. Any point P in $\mathcal{T}$ can be uniquely expressed in terms of its barycentric coordinates $\boldsymbol{\tau} = (\tau_0, \tau_1, \tau_2)$ as

$$P = \sum_{i=0}^{2} \tau_i V_i; \quad \tau_0 + \tau_1 + \tau_2 = 1,\ 0 \le \tau_i \le 1, \tag{2}$$

where τ_i, $i = 0, 1, 2$, is equal to the area of triangle (V_{i+1}, V_{i+2}, P) with i being treated cyclically modulo 3.

With $\mathbf{i} = (i, j, k)$, $|\mathbf{i}| = i + j + k$, and $i, j, k \ge 0$, let

$$B_{d;\mathbf{i}}(\boldsymbol{\tau}) := \frac{d!}{i!j!k!} \tau_1^i \tau_2^j \tau_3^k \tag{3}$$

be the *Bernstein polynomials* of degree d on $\mathcal{T}$. Then any polynomial p of total degree at most d on $\mathcal{T}$ can be expressed in the Bernstein-Bézier form

$$p(\boldsymbol{\tau}) = \sum_{|\mathbf{i}|=d} p_{\mathbf{i}} B_{d;\mathbf{i}}(\boldsymbol{\tau}). \tag{4}$$

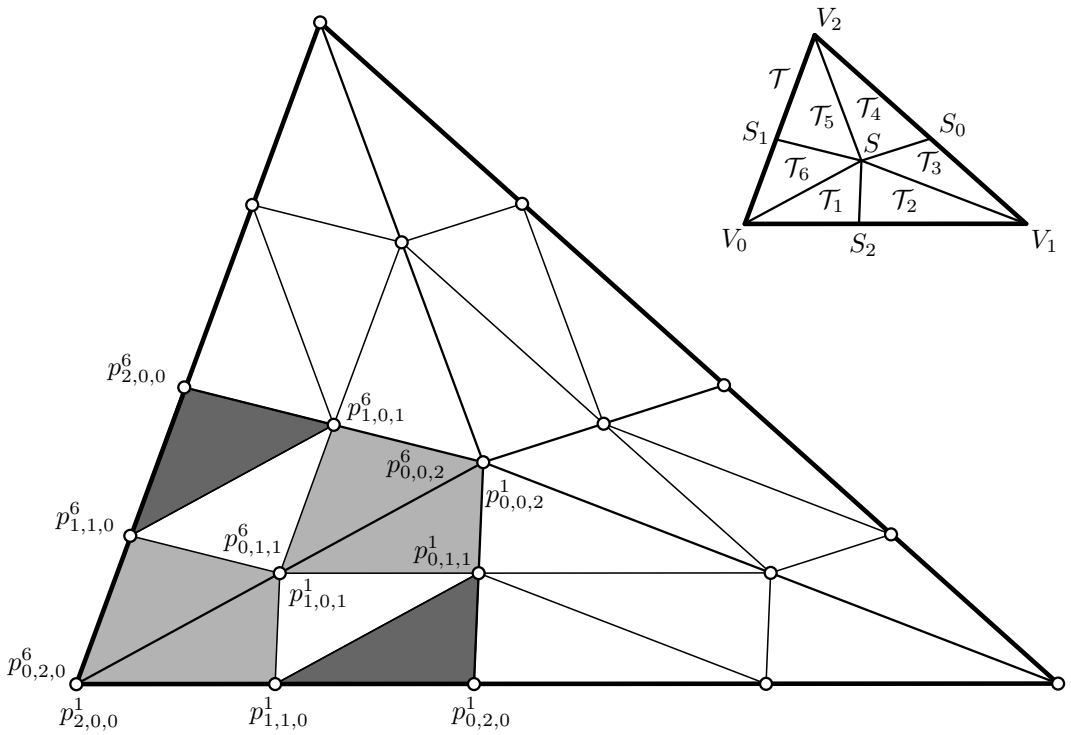

Figure 3: Labelling of Bézier ordinates (see Section 2.1) over the macro-triangle. Ordinates are labelled only over $\mathcal{T}_1$ and $\mathcal{T}_6$, others follow cyclically. The control net triangles involved in the C^1 continuity conditions (8) between p^1 and p^6 are shown in light grey, and those involved in the C^2 condition (9) are in dark grey.

These polynomials span the linear space $\Pi_d := \text{span}\{B_{d;\mathbf{i}}\}_{|\mathbf{i}|=d}$. The Bézier *ordinates* $p_\mathbf{i}$, associated with their *abscissae* $\mathbf{i}/d$ expressed in barycentric coordinates with respect to $\mathcal{T}$, form a triangular *control net* of the *Bézier triangle* (4). More details can be found in [14]. As we are dealing exclusively with quadratics ($d = 2$), we omit the d and write simply $B_\mathbf{i}$ instead of the full $B_{d;\mathbf{i}}$. Two examples of quadratic Bernstein polynomials with their control nets are shown in Figure 1.

2.2. Powell-Sabin macro-triangle and continuity conditions

The Powell-Sabin split [30] was introduced to solve the problem of bivariate Hermite interpolation over triangular meshes. Each triangle $\mathcal{T}$ of the original mesh is provided with an *inner split-point* $S \in \mathcal{T}$ and three *edge split-points* S_i, $i = 0, 1, 2$, one on each edge of $\mathcal{T}$, that introduce a segmentation of $\mathcal{T}$ into six or twelve *micro-triangles*; see Figure 2.

In this paper we focus on the 6-split macro-triangle. This split gives rise to six *micro-edges* emanating from S, three to V_i and three to S_i. The triangulation $\mathcal{T}^\star$ of $\mathcal{T}$ consisting of $\mathcal{T}_i$, $i = 1, \ldots, 6$ (see Figure 2, left) is called the *Powell-Sabin macro-triangle* (also known as *macro-element*) corresponding to $\mathcal{T}$.

The *Powell-Sabin spline space* on $\mathcal{T}^\star$ is the C^1 quadratic spline space on $\mathcal{T}^\star$, i.e.,

$$\mathcal{S}^1_2(\mathcal{T}^\star) := \{s \in C^1(\mathcal{T}^\star) : s|_{\mathcal{T}_i} \in \Pi_2, i = 1, \ldots, 6\}. \tag{5}$$

In other words, any s in $\mathcal{S}^1_2(\mathcal{T}^\star)$ consists of six quadratic Bézier triangles (one on each of the micro-triangles $\mathcal{T}_i$) joined with C^1 continuity across their pair-wise shared micro-edges. The dimension of $\mathcal{S}^1_2(\mathcal{T}^\star)$ is 9, which can be determined, for instance, using the concept of minimal determining sets [24]. A discussion on choosing the split-point S can be found in [22, 32]. Although various options exist, the split-point is typically placed at the barycentre of $\mathcal{T}$.

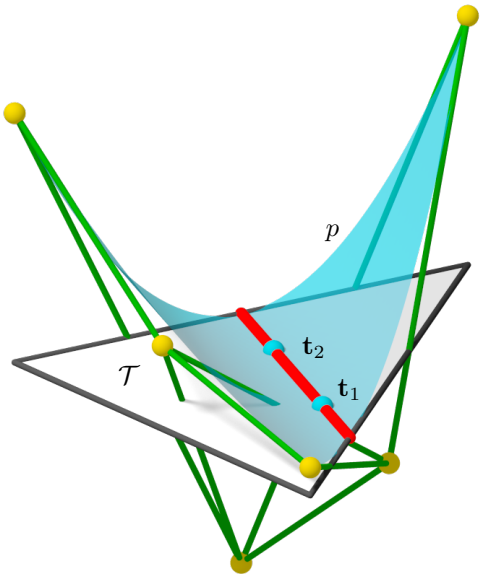

Figure 4: Two quadrature points $\mathbf{t}_1$ and $\mathbf{t}_2$ do not suffice to exactly integrate Π_2. A quadratic function $p \in \Pi_2$ over $\mathcal{T}$ that vanishes along the line $\mathbf{t}_1\mathbf{t}_2$ is shown (transparent blue). p has a non-zero integral over $\mathcal{T}$ but the integration using the quadrature rule returns zero.

We now recall C^0, C^1, and C^2 continuity conditions between quadratic Bézier triangles [23, 34]. Let p^i be a quadratic Bézier triangle defined on $\mathcal{T}_i$, $i = 1, \ldots, 6$. Using the notation from Figure 3, the C^0 continuity conditions between p^1 and p^6 at their shared micro-edge SV_0 are simply

$$p^6_{0,j,2-j} = p^1_{j,0,2-j} \quad \text{for} \quad j = 0, 1, 2. \tag{6}$$

Let the inner split-point and the edge split-points be expressed in terms of barycentric coordinates with respect to $\mathcal{T} = (V_0, V_1, V_2)$ as

$$S = (u, v, w); \quad S_0 = (0, v_0, w_0); \quad S_1 = (u_1, 0, w_1); \quad S_2 = (u_2, v_2, 0). \tag{7}$$

We assume that S is internal to $\mathcal{T}$ and all S_i are internal to their respective edges. Further, let

$$(\alpha_0, \alpha_1, \alpha_2) = \frac{1}{v_2 w}(u_1 v_2 w + u_2 w_1 v - v_2 w_1 u, -w_1 v, w_1 v_2)$$

be the barycentric coordinates of S_1 with respect to $\mathcal{T}_1 = (V_0, S_2, S)$. Then the two C^1 continuity conditions between p^1 and p^6 read

$$p^6_{1,1-j,j} = \alpha_0 p^1_{2-j,0,j} + \alpha_1 p^1_{1-j,1,j} + \alpha_2 p^1_{1-j,0,j+1} \quad \text{for} \quad j = 0, 1. \tag{8}$$

Finally, the C^2 continuity condition between p_1 and p_6 is

$$\alpha_0 p^1_{1,1,0} + \alpha_1 p^1_{0,2,0} + \alpha_2 p^1_{0,1,1} = \beta_0 p^6_{1,1,0} + \beta_1 p^6_{1,0,1} + \beta_2 p^6_{2,0,0}, \tag{9}$$

where

$$(\beta_0, \beta_1, \beta_2) = \frac{1}{w_1 v}(u_1 v_2 w + u_2 w_1 v - v_2 w_1 u, v_2 w_1, -v_2 w)$$

are the barycentric coordinates of S_2 with respect to $\mathcal{T}_6 = (V_0, S, S_1)$. More information on continuity conditions can be found e.g. in [1, 14, 23, 34].

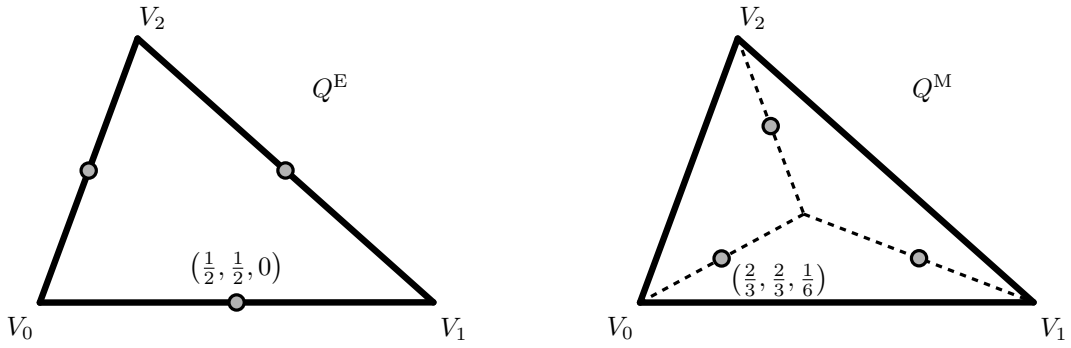

Figure 5: Two Gaussian quadrature rules for quadratic polynomials [37]. Both rules require the minimum number of quadrature points to integrate Π_2 exactly and are symmetric in terms of the barycentric coordinates defined on $\mathcal{T}$.

2.3. Gaussian quadrature for bivariate quadratic polynomials

It is known that the quadratic bivariate polynomial space requires at least three quadrature points [37]. The lower bound on the number of quadrature points is stated in general for simplices in arbitrary dimension in [37, Section 3.3]. For a two-dimensional simplex (a triangle) one can easily see that two quadrature points are not sufficient for exact integration of Π_2, see Remark 1 below. Therefore, one needs three quadrature points $\mathbf{t}_i \in \mathcal{T}$ such that

$$Q[f] := \sum_{i=1}^{3} \omega_i f(\mathbf{t}_i) = \int_{\mathcal{T}} f(\mathbf{x}) \, \mathrm{d}\mathbf{x}, \tag{10}$$

is exact for any $f \in \Pi_2$.

Remark 1. The difficulties with the existence of Gaussian quadratures for higher-dimensional simplexes can be nicely demonstrated on the example of Π_2 over triangles. Even though Π_2 is a 6-dimensional linear space over $\mathcal{T}$, there does not exist a quadrature, unlike in the univariate case, that admits exact integration using only two quadrature points, that is, the same number of degrees of freedom as the dimension of the space (two nodes in 2D and two scalar weights). A proof by contradiction goes as follows: let $\mathbf{t}_1$, $\mathbf{t}_2 \in \mathcal{T}$ be two nodes that exactly integrate Π_2, see Fig. 4. Then the quadratic function $p \in \Pi_2$ that arises by squaring a non-vanishing linear function passing through the line $\mathbf{t}_1\mathbf{t}_2$ is not integrated exactly as $Q[p] = 0$ while $\int_{\mathcal{T}} p > 0$. □

A quadrature for Π_2 of type (10), requiring three nodes, is therefore not unique. Two variants are the most common choices [37]: one prescribes the position of the nodes on the (macro-)edges, another fixes the nodes on the micro-edges from the barycentre to the vertices of the simplex. It turns out that both options lead to nodes exactly at the midpoints of their respective macro-/micro-edges. That is, the two quadratures, both exact for quadratic polynomials, read

$$Q^{\mathrm{E}}: \quad \mathbf{t}_1^{\mathrm{E}} = \left(\frac{1}{2}, \frac{1}{2}, 0\right), \quad \mathbf{t}_2^{\mathrm{E}} = \left(\frac{1}{2}, 0, \frac{1}{2}\right), \quad \mathbf{t}_3^{\mathrm{E}} = \left(0, \frac{1}{2}, \frac{1}{2}\right), \quad \omega_1^{\mathrm{E}} = \omega_2^{\mathrm{E}} = \omega_3^{\mathrm{E}} = \frac{1}{3}, \tag{11}$$

$$Q^{\mathrm{M}}: \quad \mathbf{t}_1^{\mathrm{M}} = \left(\frac{2}{3}, \frac{2}{3}, \frac{1}{6}\right), \quad \mathbf{t}_2^{\mathrm{M}} = \left(\frac{2}{3}, \frac{1}{6}, \frac{2}{3}\right), \quad \mathbf{t}_3^{\mathrm{M}} = \left(\frac{1}{6}, \frac{2}{3}, \frac{2}{3}\right), \quad \omega_1^{\mathrm{M}} = \omega_2^{\mathrm{M}} = \omega_3^{\mathrm{M}} = \frac{1}{3}, \tag{12}$$

where the nodes are described by their barycentric coordinates and the weights with respect to a triangle of unit area; see Figure 5. Regarding notation, Q^{E} stands for quadrature using nodes on (macro-)edges and Q^{M} on micro-edges. In case of the traditional 'unit' triangle with vertices at $(0, 0)$, $(1, 0)$, and $(0, 1)$, all the weights in both quadratures Q^{E} and Q^{M} are equal to $1/6$ due to the area being $1/2$.

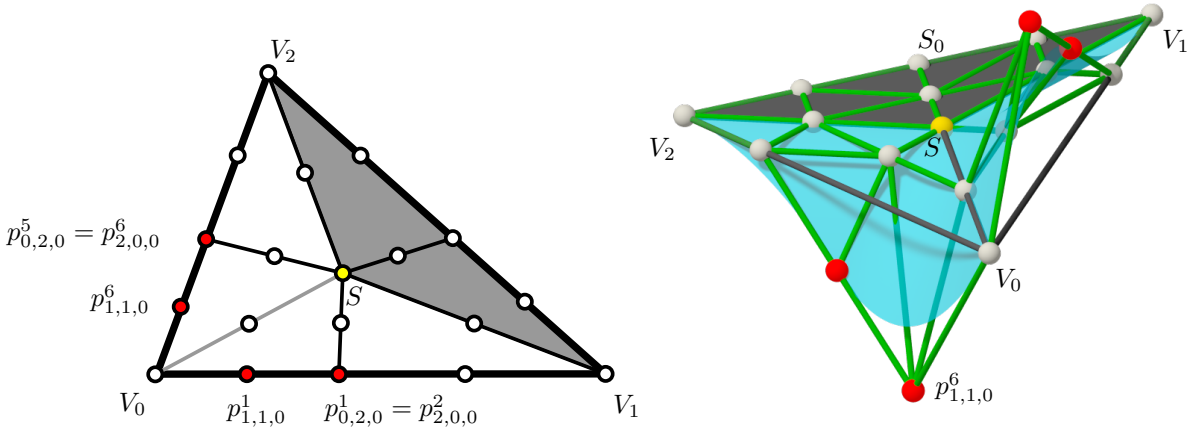

Figure 6: Left: A schematic view of the Bernstein-Bézier form of the blend D_0. The blend vanishes over the grey triangle (the union of $\mathcal{T}_3$ and $\mathcal{T}_4$) and all its Bézier ordinates are zero, except those shown in red. Right: A 3D view for the symmetric case where the split-point S (yellow) is the barycentre and the triplets V_i, S, S_i are co-linear. Again, the blend D_0 (transparent blue) vanishes over the triangle SV_1V_2 and along the edge SV_0.

3. Gaussian quadrature for C^1 quadratic Powell-Sabin macro-triangles

We study Gaussian quadrature rules for C^1 quadratic Powell-Sabin 6-split macro-triangles [30]. These macro-triangles are used in interpolation problems over triangulations, see e.g. [3, 11], and recently also in Isogeometric analysis [35]. Typically, Gaussian quadrature for quadratic polynomials (10) is used over every micro-triangle. Such integration is inefficient as it does not take advantage of the higher continuity (raised from C^{-1} to C^1) between micro-triangles. Thus we aim to find conditions when one can safely use polynomial rules also for C^1 quadratic Powell-Sabin 6-split macro-triangles, or to find efficient computational tools to numerically compute new Gaussian quadratures tailored specifically for Powell-Sabin macro-triangles.

Note that the two quadratures Q^{E} and Q^{M}, listed in (11) and (12), respectively, are *micro-edge* quadratures as defined in [21, Definition 3.1], i.e., all the nodes lie on certain micro-edges. Since there are three degrees of freedom in the polynomial quadrature rules for (total degree) quadratics using three quadrature points (see Section 2.3), a natural question arises: When and how can the polynomial rules be used (or modified) to integrate exactly also a larger space, namely the C^1 quadratic Powell-Sabin spline space over macro-triangles?

As we show below, it is the case and both rules are exact on C^1 quadratic Powell-Sabin 6-split macro-triangles when the inner split-point is the barycentre of the triangle and the edge split-points are mid-edge points.

Let the split-points be defined as in (7). Since $\dim(\mathcal{S}^1_2(\mathcal{T}^\star)) = 9$ and $\dim(\Pi_2) = 6$, we first define three spline basis functions that expand the basis of Π_2 to a basis of $\mathcal{S}^1_2$. We build these splines by blending Bernstein quadratics in a C^1 fashion.

For our purposes concerning numerical quadrature, we construct these C^1 blends D_i, $i = 0, 1, 2$ in a particular way. We require that D_0 is constant zero over $\mathcal{T}_3$ and $\mathcal{T}_4$ and that it vanishes also on micro-edge SV_0. The other two blends, D_1 and D_2, are constructed cyclically.

The case of D_0 is shown in Figure 6. Based on our specification, it is created as a blend of six Bernstein quadratics restricted to their original micro-triangles. We first define

$$\tilde{D}_0 = p^1_{1,1,0}B^1_{1,1,0}|_{\mathcal{T}_1} + p^1_{0,2,0}B^1_{0,2,0}|_{\mathcal{T}_1} + p^2_{2,0,0}B^2_{2,0,0}|_{\mathcal{T}_2} + p^6_{1,1,0}B^6_{1,1,0}|_{\mathcal{T}_6} + p^6_{2,0,0}B^6_{2,0,0}|_{\mathcal{T}_6} + p^5_{0,2,0}B^5_{0,2,0}|_{\mathcal{T}_5}. \quad (13)$$

From C^0 conditions (cf. (6)) we obtain that $p^2_{2,0,0} = p^1_{0,2,0}$ and $p^5_{0,2,0} = p^6_{2,0,0}$. The remaining four coefficients are bound by three C^1 conditions (see (8)), and are thus defined up to a multiple, as expected. Fixing

$p^1_{0,2,0} = wv_2u_2$ leads to $p^1_{1,1,0} = wv_2$, $p^6_{1,1,0} = -w_1v$, and $p^6_{2,0,0} = -w_1vu_1$.

Thus, we define

$$D_0 = wv_2B^1_{1,1,0}|_{\mathcal{T}_1} + wu_2v_2(B^1_{0,2,0}|_{\mathcal{T}_1} + B^2_{2,0,0}|_{\mathcal{T}_2}) - vw_1B^6_{1,1,0}|_{\mathcal{T}_6} - vu_1w_1(B^6_{2,0,0}|_{\mathcal{T}_6} + B^5_{0,2,0}|_{\mathcal{T}_5}). \tag{14}$$

D_1 and D_2 are defined in a similar fashion, cyclically. These three functions are C^1 and piece-wise quadratic by construction. The following lemma shows that they complement Π_2 to form a basis over the Powell-Sabin macro-element.

Lemma 3.1. *It holds that*

$$S^1_2(\mathcal{T}^\star) = \Pi_2 \oplus \operatorname{span}\{D_0, D_1, D_2\}. \tag{15}$$

Proof. As all three D_i are, by construction, in $S^1_2(\mathcal{T}^\star)$, and $\dim(\mathcal{S}^1_2(\mathcal{T}^\star)) = 9$, it only remains to show linear independence. Assume that there exists a non-trivial linear combination such that

$$c_0D_0 + c_1D_1 + c_2D_2 = \sum_{|\mathbf{i}|=2} c_{\mathbf{i}}B_{\mathbf{i}}. \tag{16}$$

As the right-hand side of (16) is a polynomial over $\mathcal{T}$ and thus C^∞, it suffices to show that the left-hand side cannot be C^2 (which is here equivalent to C^∞ since we are dealing with quadratic splines) for any c_i with $(c_0, c_1, c_2) \neq (0, 0, 0)$.

To this end, we employ the C^2 condition (9). We first apply it on micro-edge SS_1 between D_0 and D_2. As only two Bézier ordinates of D_0 and D_2 enter this C^2 condition, it in full reads $-\frac{c_0}{w_1}w_1v = \frac{c_2}{u_1}vu_1$, from which it follows that $c_0 = -c_2$. And the same argument applies to D_0 and D_1 on SS_2, yielding $c_0 = -c_1$, and also to D_1 and D_2 on SS_0, resulting in $c_1 = -c_2$. All combined, we obtain that to achieve C^2 continuity at all SS_i, it necessarily holds that $c_0 = c_1 = c_2 = 0$, as we set out to show. Note that setting all $c_{\mathbf{i}}$ to zero also proves, following the same argument, that the D_i are also mutually linearly independent. This proves (15). □

To proceed further with our investigation of Gaussian quadratures, we need to evaluate the integrals of the blends D_i over $\mathcal{T}$. Referring back to Fig. 2, the area of $\mathcal{T}_1$ is equal to v_2w, and similarly for other micro-triangles, and the integrals of all Bernstein quadratics $B_{\mathbf{i}}$ over normalised (unit area) triangles is $1/6$. Combined together with the blending coefficients in (14), we obtain

$$\begin{aligned} \textstyle\int_{\mathcal{T}} D_0 \,\mathrm{d}\mathbf{u} &= \tfrac{1}{6}(w^2v_2 - v^2w_1), \\ \textstyle\int_{\mathcal{T}} D_1 \,\mathrm{d}\mathbf{u} &= \tfrac{1}{6}(u^2w_0 - w^2u_2), \\ \textstyle\int_{\mathcal{T}} D_2 \,\mathrm{d}\mathbf{u} &= \tfrac{1}{6}(v^2u_1 - u^2v_0). \end{aligned} \tag{17}$$

Since by construction all three blends vanish along SV_i, $i = 0, 1, 2$, we now look for configurations of S, S_0, S_1, and S_2 such that the integrals of the blends vanish. Such configurations ensure that a micro-edge quadrature exact for Π_2 is also exact for $\mathcal{S}^1_2(\mathcal{T}^\star)$. Therefore, we inspect the system of equations

$$\begin{aligned} w^2v_2 - v^2w_1 &= 0, \\ u^2w_0 - w^2u_2 &= 0, \\ v^2u_1 - u^2v_0 &= 0, \end{aligned} \tag{18}$$

which contains nine variables, but only five are independent due to four linear constraints: $u + v + w = 1$, $v_0 + w_0 = 1$, $u_1 + w_1 = 1$, $u_2 + w_2 = 1$. Consequently, the system (18) is underconstrained by two variables. Due to the low degree of the system, one can solve it symbolically to get the two-parameter family of solutions

$$\begin{aligned} u_1 &= \frac{(2-2u)v + 2u - 1}{2v^2}, \\ u_2 &= \frac{2u^2 + (2v-2)u - 2v + 1}{2(1-u-v)^2}, \\ v_0 &= \frac{(2-2v)u + 2v - 1}{2u^2}, \end{aligned} \tag{19}$$

depending on the two free parameters u and v, i.e., the position of the inner split-point S. One particular solution of (19), when S is the barycentre of $\mathcal{T}$, gives the following result.

Theorem 3.1. *Let S be the barycentre of $\mathcal{T}$. Then the quadrature rule Q^{M} (12) of Hammer and Stroud is exact also for the Powell-Sabin spline space $\mathcal{S}_2^1(\mathcal{T}^\star)$ if and only if the edge split-points S_i are the midpoints of their respective edges of $\mathcal{T}$.*

Proof. The position of the inner split-point S uniquely determines the positions of S_i such that the system (18) vanishes. That is, $(u, v, w) = \left(\frac{1}{3}, \frac{1}{3}, \frac{1}{3}\right)$ gives $u_1 = u_2 = v_0 = \frac{1}{2}$ via (19).

($\Leftarrow$) If S_i, $i = 0, 1, 2$ are edge midpoints, then from (17) we have that $\int_{\mathcal{T}} D_i \,\mathrm{d}\mathbf{u} = 0$, $i = 0, 1, 2$ and, due to the construction of the blends, we also have $Q^{\mathrm{M}}[D_i] = 0$, $i = 0, 1, 2$.

($\Rightarrow$) We prove this indirectly. If one of the edge split-points is different from a midpoint, then their corresponding barycentric coordinates are not roots of system (19), and therefore at least one $\int_{\mathcal{T}} D_i \,\mathrm{d}\mathbf{u}$ does not vanish. However $Q^{\mathrm{M}}[D_i] = 0$, $i = 0, 1, 2$ and therefore (12) does not integrate $\mathcal{S}_2^1(\mathcal{T}^\star)$ exactly. □

It also follows that there exists no micro-edge quadrature of type Q^{M}, i.e., with nodes on the micro-edges SV_i, $i = 0, 1, 2$, which is exact on $\mathcal{S}_2^1(\mathcal{T}^\star)$ when the split-point is the barycentre of $\mathcal{T}$ and at least one of the edge split-points is not the midpoint of its corresponding edge. Indeed, in such a configuration at least one of the integrals in (17) does not vanish, yet such micro-quadrature gives zero results for all the blends D_i, $i = 0, 1, 2$, due to the construction of the blends: they all vanish on the three micro-edges SV_i, $i = 0, 1, 2$.

We now show an analogous result to Theorem 3.1 for Q^{E}.

Theorem 3.2. *Let S be the barycentre of $\mathcal{T}$. Then the quadrature rule Q^{E} (11) of Hammer and Stroud is exact also for the Powell-Sabin spline space $\mathcal{S}_2^1(\mathcal{T}^\star)$ if and only if the edge split-points S_i are midpoints of their respective edges of $\mathcal{T}$.*

Proof. ($\Leftarrow$) Assume that S_i, $i = 0, 1, 2$ are edge midpoints. Then $D_0(S_0) = 0$, $D_0(S_1) = -1/12$, and $D_0(S_2) = 1/12$, and thus $Q^{\mathrm{E}}[D_0] = 0$. By cyclic symmetry, also $Q^{\mathrm{E}}[D_1]$ and $Q^{\mathrm{E}}[D_2]$ vanish. At the same time, $\int_{\mathcal{T}} D_i \,\mathrm{d}\mathbf{u} = 0$, $i = 0, 1, 2$, which shows exactness of Q^{E} on $\mathcal{S}_2^1(\mathcal{T}^\star)$ in the fully symmetric case.

($\Rightarrow$) Assume that Q^{E} is exact on $\mathcal{S}_2^1(\mathcal{T}^\star)$ with S at the barycentre of $\mathcal{T}$, i.e., $\int_{\mathcal{T}} D_i \,\mathrm{d}\mathbf{u} = Q^{\mathrm{E}}[D_i]$ for $i = 0, 1, 2$. From (14) it follows that

$$D_0(S_0) = 0, \qquad D_0(S_1) = \frac{1}{12} \cdot \begin{cases} \frac{u_1}{u_1 - 1} & u_1 \le \frac{1}{2} \\ \frac{1 - 3u_1}{u_1} & u_1 \ge \frac{1}{2} \end{cases}, \qquad D_0(S_2) = \frac{1}{12} \cdot \begin{cases} \frac{v_2}{1 - v_2} & v_2 \le \frac{1}{2} \\ \frac{3v_2 - 1}{v_2} & v_2 \ge \frac{1}{2} \end{cases}.$$

This in turn, combined with the first equation in (17), leads to

$$Q^{\mathrm{E}}[D_0] = \frac{1}{12} \cdot \begin{cases} \frac{u_1}{u_1 - 1} & u_1 \le \frac{1}{2} \\ \frac{1 - 3u_1}{u_1} & u_1 \ge \frac{1}{2} \end{cases} + \frac{1}{12} \cdot \begin{cases} \frac{v_2}{1 - v_2} & v_2 \le \frac{1}{2} \\ \frac{3v_2 - 1}{v_2} & v_2 \ge \frac{1}{2} \end{cases} = \frac{1}{6}(w^2 v_2 - v^2 w_1) = \int_{\mathcal{T}} D_0 \,\mathrm{d}\mathbf{u},$$

which expresses the exactness of Q^{E} on D_0. Similar equations, again exploiting cyclic symmetry, are obtained for D_1 and D_2. Thus, we obtain three piece-wise polynomial equations which are cubic in u_1, v_2, and w_0; cf. (7). Using a computer algebra system such as Maple, it can be shown that this system, in all its eight polynomial variants based on the ranges of u_1, v_2, and w_0, admits only one solution: $u_1 = v_2 = w_0 = 1/2$, as we set out to prove. □

One could still ask whether it is possible to move the nodes of Q^{E} along the edges of $\mathcal{T}$ to integrate $\mathcal{S}_2^1(\mathcal{T}^\star)$ exactly when the edge split-points are not midpoints. The answer is negative: Q^{E} is the only three-node quadrature exact on Π_2 over $\mathcal{T}$ having its nodes on the edges of $\mathcal{T}$.

We now move on to the more challenging case of non-symmetric splits.

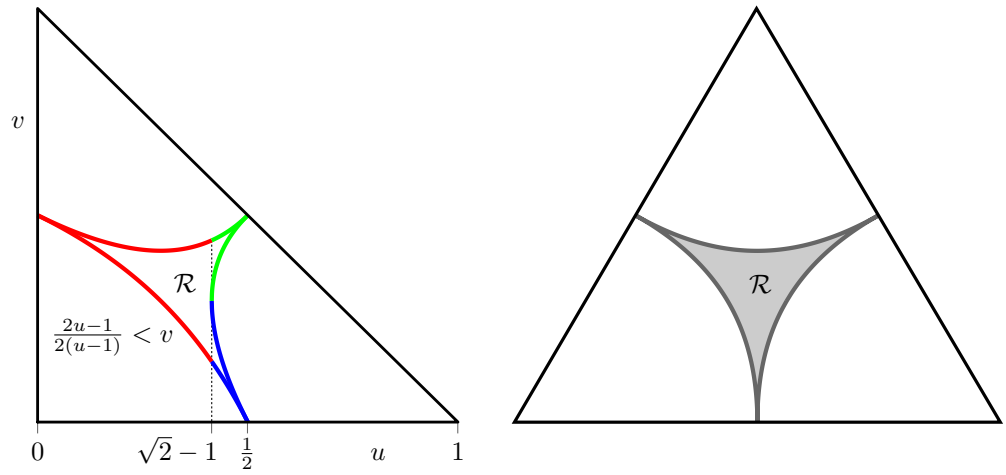

Figure 7: Two visualisations of the region $\mathcal{R}$ of all admissible inner split-points S ensuring the existence of a micro-edge quadrature of type Q^{M} for $\mathcal{S}_2^1(\mathcal{T}^\star)$. Left: The triangular domain shown in standard Cartesian coordinates, which allows for a direct interpretation of the inequalities in (20) in order red, blue, and green. The bounding curves of $\mathcal{R}$ are hyperbolic arcs. Right: $\mathcal{R}$ visualised (in grey) in the symmetric situation where the domain triangle of barycentric coordinates is equilateral.

3.1. Gaussian quadrature for non-symmetric Powell-Sabin splits

The choice of the barycentre as the inner split-point is very natural and is the typical choice in applications [30, 32], and Theorems 3.1 and 3.2 address the special situation where the edge split-points are edge mid-points. However, the theory of quadratic spline approximation works for arbitrary split-points [30] and we are now interested in to what extent one can adapt the polynomial quadrature rules for the Powell-Sabin splines with general split-points.

The symbolic solution in (19) corresponds to the exactness of some micro-edge quadrature rule of $\mathcal{S}_2^1(\mathcal{T}^\star)$ and the solution triplet (u_1, u_2, v_0) determines the positions of the edge split-points S_i, $i = 0, 1, 2$. In order to be well defined, the edge split-points have to lie on their corresponding edges. The solution in (19) depends on two parameters, u and v, which in turn determine the position of S. And thus we ask: What is the admissible region for S such that the edge split-points given by (19) are well defined? In other words, we want to find the locus $\mathcal{R}$ of S for which $0 < u_1, u_2, v_0 < 1$. These constraints give rise to the following inequalities

$$\begin{aligned}
\frac{2u-1}{2(u-1)} &< v < \frac{(2u^2-2u+1)}{2(1-u)}, && u \in [0, \sqrt{2}-1], \\
\frac{2u-1}{2(u-1)} &< v < \frac{(1-u-\sqrt{u^2+2u-1})}{2}, && u \in [\sqrt{2}-1, \tfrac{1}{2}], \\
\frac{(1-u+\sqrt{u^2+2u-1})}{2} &< v < \frac{2u-2u^2-1}{2(u-1)}, && u \in [\sqrt{2}-1, \tfrac{1}{2}]
\end{aligned} \tag{20}$$

defining $\mathcal{R}$; see Fig. 7. Choosing $S \in \mathcal{R}$ guarantees that there exist edge split-points S_i inside $V_{i+1}V_{i+2}$ such that (19) holds.

Let us consider $(u, v) \in \mathcal{R}$. By construction, any micro-edge quadrature will exactly integrate the three blends D_i, because $\int_{\mathcal{T}} D_i \,\mathrm{d}\mathbf{u} = Q[D_i] = 0$. To construct a micro-edge quadrature rule that is exact for $\mathcal{S}_2^1(\mathcal{T}^\star)$, it is therefore sufficient to find three nodes on micro-edges SV_i, one on each, and the corresponding weights that exactly integrate Π_2. This leads to a well-constrained (6×6) polynomial system

$$\int_{\mathcal{T}} B_{\mathbf{i}} \,\mathrm{d}\mathbf{u} = Q(t_1, t_2, t_3, \omega_1, \omega_2, \omega_3)[B_{\mathbf{i}}], \quad |\mathbf{i}| = 2, \tag{21}$$

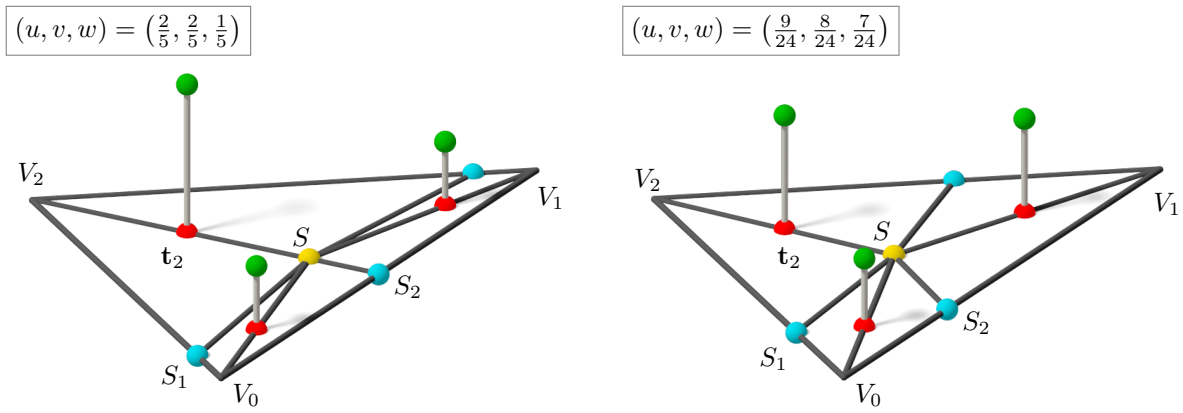

Figure 8: Two micro-edge Gaussian quadrature rules for $\mathcal{S}_2^1(\mathcal{T}^\star)$. The inner split-point (yellow) is chosen from the admissible region $\mathcal{R}$ (see Fig. 7) and the boundary split-points (blue) are computed using (19). The nodes of the micro-edge (red) and weights (visualised as the distances between green and red bullets) were computed numerically via (21) using (12) as the initial guess.

where $B_{\mathbf{i}}$ are the quadratic Bernstein-Bézier basis functions of Π_2 (see Section 2.1). The unknowns t_i represent the micro-edge quadrature nodes $\mathbf{t}_i = (1-t_i)S + t_i V_i$ and ω_i are their associated weights.

While a symbolic solution of this system for an arbitrary split-point exists (parametrised by u and v), it has an excessive number of terms and is thus impractical. (Although we can provide this to an interested reader as a Maple worksheet.) So instead, we opted for the more practical numerical approach to compute particular quadrature rules. Specifically, we used the Newton-Raphson method with the micro-edge Hammer and Stroud rule (12) as the initial guess. This was implemented in Maple and numerical precision was set to 20 digits.

Two particular Gaussian rules for $\mathcal{S}_2^1(\mathcal{T}^\star)$ are shown in Fig. 8. The rules are determined by the position of the inner split-point S. While a median-symmetric position of S yields a rule that is symmetric, as depicted in Fig. 8, left, the rule is in general non-symmetric, as shown in Fig. 8, right.

To numerically validate the results, we tested the two rules shown in Table 1 by computing the error

$$\varepsilon(f) = Q[f] - \int_{\mathcal{T}} f \, \mathrm{d}\mathbf{u} \tag{22}$$

for functions $f \in \mathcal{S}_2^1(\mathcal{T}^\star)$. Observe that, by construction, the rules are exact for the blends D_i, $i = 0, 1, 2$. Therefore, we sample only $f \in \Pi_2$ and compute $\varepsilon(f)$. The quadrature rules were computed with the precision of 20 decimal digits. Three test functions and their errors are shown in Fig 9.

An example of evolution of the Gaussian rules for $\mathcal{S}_2^1(\mathcal{T}^\star)$ is shown in Fig. 10. The split-point S starts from the barycentre of $\mathcal{T}$ (time $t = 0$) and moves straight towards a vertex until it reaches the boundary of

Table 1: The two micro-edge Gaussian quadrature rules for the Powell-Sabin micro-triangles shown in Fig. 8. The barycentric coordinates of S, (u, v, w), define the boundary split-points via (19). The positions of the quadrature points $\mathbf{t}_i$ are determined by t_i, the barycentric coordinate on the micro-edge SV_i, i.e., $\mathbf{t}_i = (1-t_i)S + t_i V_i$.

(u,v,w)	i	t_i	ω_i
$\left(\frac{2}{5}, \frac{2}{5}, \frac{1}{5}\right)$	0	0.59910635852267947645	0.23217256322315208284
	1	0.59910635852267947645	0.23217256322315208284
	2	0.44098300562505257589	0.53565487355369583432
$\left(\frac{9}{24}, \frac{8}{24}, \frac{7}{24}\right)$	0	0.59012269252438973205	0.24784153484760864812
	1	0.49095437891053568222	0.34024176149379593418
	2	0.45598891682541458848	0.41191670365859541770

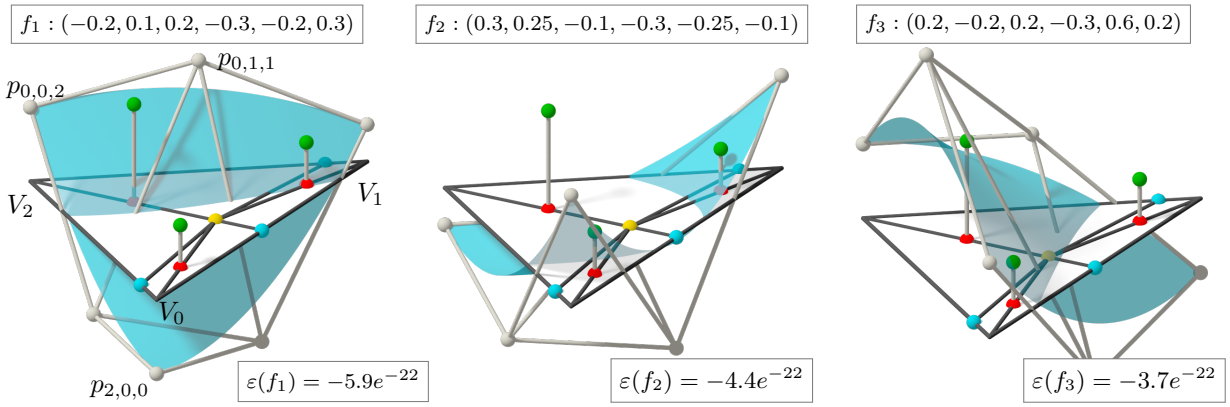

Figure 9: Three polynomials $f_i \in \Pi_2$, $i = 1, 2, 3$, with the corresponding vectors of Bernstein-Bézier control net coefficients $(p_{2,0,0}, p_{0,2,0}, p_{0,0,2}, p_{0,1,1}, p_{1,0,1}, p_{1,1,0})$ are shown. The error values, see (22), between the exact integrals and the results of the quadrature rule (red/green bullets; Table 1, top) are displayed.

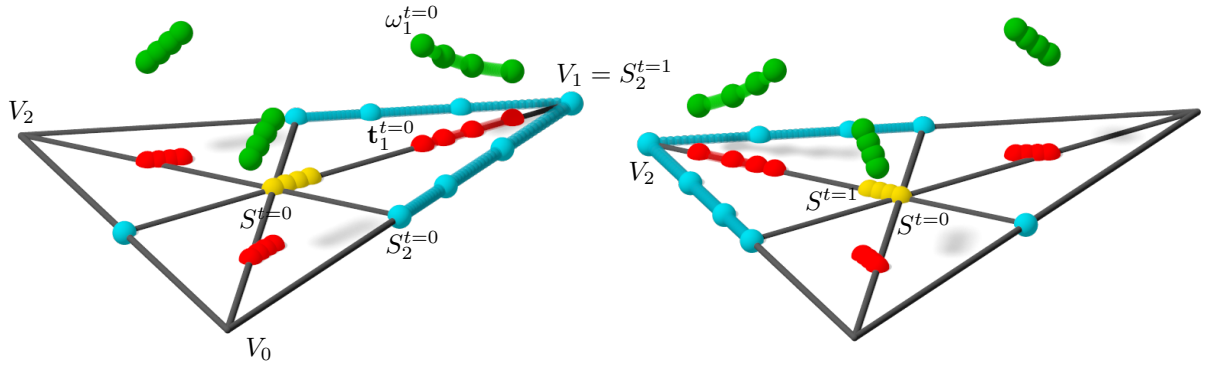

Figure 10: Evolution of the Gaussian rules. Left: The split-point (yellow) is being moved from its original position at time $t = 0$, $S^{t=0}$, towards the vertex V_1 until it reaches the boundary of the admissible region (cf. Fig. 7) at time $t = 1$. The trajectories of the nodes (red) and weights (green) are traced numerically. The position of the edge split-points S_i are governed by (19). The edge split-point opposite the target vertex remains constant at its edge midpoint. Right: Evolution of the rule as S moves towards V_2.

the admissible region $\mathcal{R}$, see Fig. 7, at time $t = 1$. For each particular time instant, the edge split-points S_i are computed directly from (19), and the nodes $\mathbf{t}_i$ and weights ω_i, $i = 1, 2, 3$, are traced numerically.

3.2. Discussion and limitations

We have analysed Gaussian quadrature rules for C^1 quadratic Powell-Sabin 6-split macro-elements, focusing on the fully symmetric case. We have shown that in the fully symmetric configuration, the two quadratures, Q^{E} in (11) and Q^{M} in (12), of Hammer and Stroud for quadratic polynomials also integrate exactly the Powell-Sabin space $\mathcal{S}_2^1(\mathcal{T}^\star)$ over a macro-triangle $\mathcal{T}$, and the number of nodes (three) is optimal.

Number of nodes needed for	Q^{E}	Q^{M}	asympt. Q^{E}	asympt. Q^{M}
micro-triangle integration	6T + 2E	18T	6E	12E
macro-triangle integration	E	3T	E	2E

Table 2: The number of nodes needed when using different quadrature rules on a triangulation with T triangles and E edges, and when used per micro-triangle or per macro-triangle. The last two columns list the asymptotic node counts for $2E \approx 3T$.

Consequently, the number of required nodes is only three, in contrast to the classical polynomial rules which involve twelve nodes in the case of (11) or even eighteen for (12) when used per micro-triangle.

This result generalises to regular, fully symmetric triangulations, although the combined rule is no longer optimal. Nevertheless, it still results in considerable quadrature node savings. Table 2 compares our results on an input triangulation with T triangles and E edges. Asymptotically, a regular triangulation with a large number of elements satisfies $2E \approx 3T$. Table 2 then clearly shows that the Q^{E} rule uses the minimal number of nodes among all the investigated exact quadratures.

In Section 3.1, we attacked the problem of extending our results to non-symmetric macro-triangles, which turned out to be a formidable problem. Solving the fully general system of polynomial equations to find a quadrature for $\mathcal{S}_2^1(\mathcal{T}^\star)$ parametrised by the positions of S and S_i, $i = 0, 1, 2$, is beyond the current capacity of computer algebra systems. Our numerical tests, such as those shown in Figs. 8 and 10, and many other tests we performed, indicate that three nodes suffice also in the general situation. However, a rigorous proof of this fact is yet to be found, ideally combined with an efficient algorithm or even a closed-form formula for computing the underlying quadrature nodes and weights on general triangulations and 6-splits.

Our quadrature rules are, up to machine precision, exact for $\mathcal{S}_2^1(\mathcal{T}^\star)$ and thus a natural question arises: What is the integration error if $f \notin \mathcal{S}_2^1(\mathcal{T}^\star)$? We see such error analysis, even for a particular spline space determined by a given split-point S, as rather complicated. However, as $\Pi_2 \subset \mathcal{S}_2^1(\mathcal{T}^\star)$, one may use the error estimates for polynomials [37, Chapter 5]. These estimates are mainly formulated over rectangular domains, and therefore embedding $\mathcal{T}$ into a corresponding rectangle and using the bounds from [37, Section 5.3] over each triangle gives conservative error estimates for our rules.

4. Conclusion

We have investigated Gaussian quadrature rules for C^1 quadratic Powell-Sabin 6-split macro-triangles. We have shown that for the inner split-point at the barycentre, the two 3-node micro-edge quadratures for quadratic polynomials of Hammer and Stroud generalise to the Powell-Sabin 6-split macro-element space if and only the edge split-points are the midpoints of their respective edges. Our result describes special Powell-Sabin 6-splits that require only three quadrature points per macro-triangle, in contrast to classical polynomial rules that require twelve nodes. The existence of other (micro-edge) quadratures as well as the generalisation of the rules from the case of a single macro-triangle to a whole triangular mesh remain open problems for future research.

Acknowledgements. The first author has been partially supported by the Basque Government through the BERC 2014-2017 program, by Spanish Ministry of Economy and Competitiveness MINECO: BCAM Severo Ochoa excellence accreditation SEV-2013-0323, and the Project of the Spanish Ministry of Economy and Competitiveness with reference MTM2016-76329-R (AEI/FEDER, EU).

[1] P. Alfeld and L. Schumaker. Smooth macro-elements based on Clough-Tocher triangle splits. *Numerische Mathematik*, 90(4):597–616, 2002.

[2] F. Auricchio, F. Calabrò, T. J. R. Hughes, A. Reali, and G. Sangalli. A simple algorithm for obtaining nearly optimal quadrature rules for NURBS-based isogeometric analysis. *Computer Methods in Applied Mechanics and Engineering*, 249-252(1):15–27, 2012.

[3] R. E. Barnhill. Surfaces in computer aided geometric design: A survey with new results. *Computer Aided Geometric Design*, 2(1-3):1–17, 1985.

[4] M. Bartoň, R. Ait-Haddou, and V. M. Calo. Gaussian quadrature rules for C^1 quintic splines with uniform knot vectors. *Journal of Computational and Applied Mathematics*, 322:57–70, 2017.

[5] M. Bartoň and V. Calo. Gaussian quadrature for splines via homotopy continuation: rules for C^2 cubic splines. *Journal of Computational and Applied Mathematics*, 296:709–723, 2016.

[6] M. Bartoň and V. Calo. Gauss-Galerkin quadrature rules for quadratic and cubic spline spaces and their application to isogeometric analysis. *Computer-Aided Design*, 82:57–67, 2017.

[7] F. Calabrò, A. Falini, M. L. Sampoli, and A. Sestini. Efficient quadrature rules based on spline quasi–interpolation for application to iga-bems. *Journal of Computational and Applied Mathematics*, 2018.

[8] F. Calabrò, G. Sangalli, and M. Tani. Fast formation of isogeometric Galerkin matrices by weighted quadrature. *Computer Methods in Applied Mechanics and Engineering*, 2016.

[9] R. W. Clough and J. L. Tocher. Finite element stiffness matrices for analysis of plates in bending. In *Conference on Matrix Methods in Structural Mechanics*, pages 515–545. Wright Patterson Air Force Base, Ohio, 1965.
[10] J. Cottrell, T. Hughes, and Y. Bazilevs. *Isogeometric Analysis: Toward Integration of CAD and FEA*. John Wiley & Sons, 2009.
[11] M. Dæhlen, T. Lyche, K. Mørken, R. Schneider, and H.-P. Seidel. Multiresolution analysis over triangles, based on quadratic hermite interpolation. *Journal of Computational and Applied Mathematics*, 119(1):97–114, 2000.
[12] C. Dagnino and P. Lamberti. Numerical integration of 2D integrals based on local bivariate c^1 quasiinterpolating splines. *Advances in Computational Mathematics*, 8(1):19–31, Jan 1998.
[13] C. de Boor, K. Höllig, and S. Riemenschneider. *Box splines*. Springer, New York, 1993.
[14] G. Farin. Triangular Bernstein-Bézier patches. *Computer Aided Geometric Design*, 3(2):83–127, 1986.
[15] G. H. Golub and J. H. Welsch. Calculation of Gauss quadrature rules. *Mathematics of Computation*, 106(23):221 – 230, 1969.
[16] P. C. Hammer and A. H. Stroud. Numerical integration over simplexes. *Mathematical tables and other aids to computation*, 10(55):137–139, 1956.
[17] R. R. Hiemstra, F. Calabrò, D. Schillinger, and T. J. Hughes. Optimal and reduced quadrature rules for tensor product and hierarchically refined splines in isogeometric analysis. *Computer Methods in Applied Mechanics and Engineering*, 316:966–1004, 2017.
[18] F. Hildebrand. *Introduction to Numerical Analysis*. McGraw-Hill, New York, 1956.
[19] T. Hughes, A. Reali, and G. Sangalli. Efficient quadrature for NURBS-based isogeometric analysis. *Computer Methods in Applied Mechanics and Engineering*, 199(58):301 – 313, 2010.
[20] K. A. Johannessen. Optimal quadrature for univariate and tensor product splines. *Computer Methods in Applied Mechanics and Engineering*, 316:84–99, 2017.
[21] J. Kosinka and M. Bartoň. Gaussian quadrature for C^1 cubic Clough-Tocher macro-triangles. *submitted to Foundations of Computational Mathematics*. preprint available at `http://www.cs.rug.nl/~jiri/papers/17KoBa.pdf`.
[22] J. Kosinka and T. J. Cashman. Watertight conversion of trimmed CAD surfaces to Clough-Tocher splines. *Computer Aided Geometric Design*, 37:25–41, 2015.
[23] M. Lai and L. Schumaker. Macro-elements and stable local bases for splines on Clough-Tocher triangulations. *Numerische Mathematik*, 88(1):105–119, 2001.
[24] M. Lai and L. Schumaker. *Spline Functions on Triangulations*. Cambridge University Press, 2007.
[25] P. Lamberti. Numerical integration based on bivariate quadratic spline quasi-interpolants on bounded domains. *BIT Numerical Mathematics*, 49(3):565–588, Sep 2009.
[26] J. N. Lyness and R. Cools. A survey of numerical cubature over triangles. Technical report, Mathematics and Computer Science Division, Argonne National Laboratory, 1994. III, MCS-P410-0194.
[27] J. Ma, V. Rokhlin, and S. Wandzura. Generalized Gaussian quadrature rules for systems of arbitrary functions. *SIAM Journal on Numerical Analysis*, 33(3):971–996, 1996.
[28] S. Mousavi, H. Xiao, and N. Sukumar. Generalized Gaussian quadrature rules on arbitrary polygons. *International Journal for Numerical Methods in Engineering*, 82(1):99–113, 2010.
[29] G. Nikolov. Asymptotically optimal definite quadrature formulae. *ZAMM SII*, 75:653 – 654, 1995.
[30] M. J. D. Powell and M. A. Sabin. Piecewise quadratic approximations on triangles. *ACM Trans. Math. Softw.*, 3(4):316–325, Dec. 1977.
[31] P. Sablonnière, D. Sbibih, and M. Tahrichi. Numerical integration based on bivariate quadratic spline quasi-interpolants on Powell-Sabin partitions. *BIT Numerical Mathematics*, 53(1):175–192, Mar 2013.
[32] L. L. Schumaker and H. Speleers. Nonnegativity preserving macro-element interpolation of scattered data. *Computer Aided Geometric Design*, 27(3):245–261, 2010.
[33] I. H. Sloan. A quadrature-based approach to improving the collocation method. *Numerische Mathematik*, 54(1):41 – 56, 1988.
[34] H. Speleers. A normalized basis for reduced Clough-Tocher splines. *Computer Aided Geometric Design*, 27(9):700–712, 2010.
[35] H. Speleers and C. Manni. Optimizing domain parameterization in isogeometric analysis based on Powell-Sabin splines. *Journal of Computational and Applied Mathematics*, 289:68–86, 2015. Sixth International Conference on Advanced Computational Methods in Engineering (ACOMEN 2014).
[36] A. Stroud and D. Secrest. *Gaussian Quadrature Formulas*. Prentice-Hall, Englewood Cliffs, N.J., 1966.
[37] A. H. Stroud. *Approximate calculation of multiple integrals*. Prentice-Hall, 1971.
[38] J. Van Deun, A. Bultheel, and P. González Vera. On computing rational gauss-chebyshev quadrature formulas. *Mathematics of Computation*, 75(253):307–326, 2006.
[39] H. Xiao and Z. Gimbutas. A numerical algorithm for the construction of efficient quadrature rules in two and higher dimensions. *Computers & mathematics with applications*, 59(2):663–676, 2010.